CrossMark

ORIGINAL RESEARCH

Double inversion recovery imaging improves the evaluation of gray matter volume losses in patients with Alzheimer's disease and mild cognitive impairment

Geon-Ho Jahng[1] · Dong Kyun Lee[2] · Jong-Min Lee[2] · Hak Young Rhee[3] · Chang-Woo Ryu[1]

Abstract Our goal was to investigate whether three-dimensional (3D) double inversion recovery (DIR) images can show alterations of gray matter volume (GMV) between Alzheimer's disease (AD) patients and nondemented controls and to compare alterations of GMV between groups using DIR images and those using 3D T1-weighted (T1W) images. We included 25 subjects with mild or probable AD, 25 subjects with amnestic mild cognitive impairment (MCI), and 25 elderly cognitively normal (CN) subjects. Group differences in GMV among CN, MCI, and AD patients were tested by voxel-wise, one-way ANOVA. Additional region-of-interest-based comparisons of GMV differences among the three groups for DIR and T1WI were performed using ANCOVA. Finally, ROC curve analysis was performed. In the AD group compared with the CN and MCI groups, GMV was decreased in both DIR and T1W images. However, the areas showing GMV loss were larger in DIR images compared to those in T1W images. Amygdala had the highest area under curve value for both DIR and T1W images. DIR images were sensitive for identifying GMV loss in patients with AD compared with MCI and CN subjects and areas showing GMV loss identified with DIR were extended to more brain areas than those identified with T1W. With DIR, amygdala GMV is the most sensitive in differentiating between subject groups.

Keywords Magnetic resonance imaging · Double inversion recovery · Gray matter volume · Alzheimer's disease · Amygdala

✉ Geon-Ho Jahng
ghjahng@gmail.com

[1] Department of Radiology, Kyung Hee University Hospital at Gangdong, College of Medicine, Kyung Hee University, #892 Dongnam-ro, Gangdong-gu, Seoul 134-727, Republic of Korea

[2] Computational NeuroImage Analysis Lab, Department of Biomedical Engineering, Hanyang University, Sungdong P.O. Box 55, Seoul 133-605, Republic of Korea

[3] Department of Neurology, Kyung Hee University Hospital at Gangdong, College of Medicine, Kyung Hee University, #892 Dongnam-ro, Gangdong-gu, Seoul 134-727, Republic of Korea

Introduction

Alzheimer's disease (AD) is characterized by the progressive deterioration of cognitive functions, and changes in behaviors and the ability to carry out daily activities (Good et al. 2002). Mild cognitive impairment (MCI) often represents a transitional state between normal aging and dementia (Small et al. 2008) and is a high-risk condition for the development of clinically probable AD (Petersen et al. 1999). The reliable diagnosis of MCI in cases can be the key point in AD prevention. Differentiation of MCI from AD is also important, since not all cases of MCI will convert to AD.

Structural magnetic resonance imaging (MRI) can detect subtle brain atrophy as a surrogate marker for pathological processes in AD. A three-dimensional (3D) T1-weighted (T1W) image is usually used to evaluate brain atrophy by using voxel-based morphometry (VBM) (Ashburner and Friston 2000) which is potentially helpful to evaluate regional gray matter volume (GMV) differences between controls and AD patients (Baron et al. 2001). Previous VBM studies of GMV in AD showed regional gray matter atrophy in the

Springer

temporal lobes of the brain, extending to the frontal and parietal lobes with progression of the disease (Bozzali et al. 2006). 3D T1W images are used as a gold standard to evaluate brain atrophy. However, evaluation of brain tissue volume on the 3D T1W image is dependent on the result of brain tissue segmentation and is also subjective to the partial volume effect (PVE), resulting in inaccuracy of both qualitative and quantitative assessments. A voxel-related complication is PVE, wherein a single voxel can contain variable amounts of gray matter, white matter, and cerebrospinal fluid (CSF). The structural 3D T1W image of the brain is usually obtained with an inversion radiofrequency pulse to eliminate signals from CSF. Although the PVE can be reduced by reducing the voxel size, it should be beneficial for suppressing both white matter and CSF while leaving gray matter to minimize the PVE.

A double inversion recovery (DIR) imaging sequence was introduced to simultaneously suppress the signals from both CSF and normal white matter in the brain with the application of two 180° inversion pulses before readout data by selecting two suitable inversion times, allowing better visualization of the remaining tissues, although DIR may have a flow-related artifact (Redpath and Smith 1994). DIR reduces partial volume effects of gray matter with white matter and CSF. Pouwels et al. investigated feasibility of 3D DIR images to evaluate gray matter signal intensity and they gave an idea of potential usefulness of 3D DIR to determine cortical thickness and gray matter volume (Pouwels et al. 2006).

There is no study that evaluated gray matter volume changes in AD with DIR. Therefore, the objectives of this study were 1) to prospectively investigate whether DIR images can show alterations of GMV in AD patients compared with nondemented controls and 2) to compare alterations of GMV between groups using DIR images and those using 3D T1W images. We hypothesized that GMV losses in AD subjects can be depicted by DIR images with improved sensitivity for differentiating AD patients from MCI or CN subjects.

Materials and methods

Subjects

Our institutional review board approved this study and informed consent was obtained from all participants. All participants provided a detailed medical history and underwent a neurologic examination, standard neuropsychological testing, and magnetic resonance imaging (MRI) scan. Cognitive function was assessed by application of the Seoul Neuropsychological Screening Battery (SNSB) which is a standardized full neuropsychological battery in Korea that comprises tests for specific cognitive domains (Ahn et al. 2010). A neuroradiologist with 6 years of imaging experience evaluated brain MR images of each subject to detect any evidence of prior cortical infarctions

or other space-occupying lesions. The MCI criteria were based on Petersen's criteria as follows: (1) cognitive complaints by patient or caregiver; (2) normal general cognitive function on the Korean version of the Mini-Mental State Examination (K-MMSE); (3) cognitive impairment on objective testing; (4) normal activities of daily living; and (5) no dementia (Petersen et al. 2001; Petersen et al. 1999). We included mild and probable AD patients who met the criteria of National Institute of Neurological and Communicative Disorders and Stroke-Alzheimer disease and Related Disorders Association (McKhann et al. 1984): (1) dementia established by clinical examination and standardized brief mental status examination and confirmed by neuropsychological tests; (2) deficits in two or more areas of cognition; (3) progressive worsening of memory and other cognitive functions; (4) no disturbance of consciousness; (5) onset between 40 and 90 years; and (6) absence of other systemic or neurologic disorders sufficient to account for the progressive cognitive defects. Based on the results of SNSB examination and MRI findings, we included 25 cognitively normal (CN) subjects who did not have a medical history of neurological disease and who showed normal results on detailed cognitive testing and brain MRI, 25 subjects with amnestic MCI, and 25 subjects with mild or probable AD. Demographic characteristics and results of neuropsychological tests are summarized in Table 1.

Image acquisition

Images were acquired with a 3 Tesla MRI scanner (Achieva, Philips Medical System, Best, The Netherlands) using a

Table 1 Demographic data and neuropsychological test results

	AD	MCI	CN
Subjects	25	25	25
Age (years)[a]	70.9 ± 9.8	67.6 ± 7.4	68.4 ± 5.6
Gender[b]			
male	4	12	9
female	21	13	16
MMSE[c]	17.2 ± 4.7	26.8 ± 3.5	27.3 ± 2.8

Data for age and MMSE are presented as mean ± standard deviation

AD Alzheimer's disease

MCI Mild Cognitive Impairment

CN Cognitively Normal

MMSE Mini Mental State Examination Score

[a] Age was not significantly different among the groups ($P > 0.05$)

[b] Gender was not significantly different between the CN group and the other two groups ($P > 0.05$), but it was significantly different between the MCI and AD groups ($P < 0.05$)

[c] MMSE scores were significantly different between the AD group and the other two groups ($P < 0.05$), but the scores were not different between the MCI and CN groups ($P > 0.564$)

dedicated 8-element phased array sensitivity-encoding (SENSE) head coil. The 3D DIR sequence consisted of two 180° inversion radiofrequency (RF) pulses preceding the turbo spin-echo (TSE) imaging acquisition (Turetschek et al. 1998; Meara and Barker 2005). The aim was to suppress the signals from both normal white matter and CSF to obtain an image of the distribution of the gray matter. We used the first inversion time (TI_1) of 2930 ms to suppress CSF signals, assuming a longitudinal relaxation time (T1) of 4300 ms in CSF and a second inversion time (TI_2) of 350 ms to suppress the white matter signals, assuming T1 = 830 ms in white matter of human brain in a 3 Tesla MRI system (Redpath and Smith 1994; Boulby et al. 2004). The effective echo time (TE) was 100 ms. The excitation 90° radiofrequency pulse was preceded by a fat saturation pulse using the spectral pre-saturation with inversion recovery (SPIR) method and an inferiorly placed saturation slab to minimize flow artifacts. Additional imaging parameters for the transverse 3D DIR sequence were: repetition time (TR)/TE = 8000/100 ms, echo-spacing =10.2 ms, echo-train length = 11, overcontiguous slice thickness = 4 mm and reconstructed slice thickness = 2 mm, acquisition matrix =256 × 163 and reconstructed matrix =512 × 512, field of view (FOV) = 230 mm × 183 mm, number of slices =50, acquisition voxel size = 0.9 × 1.12 × 4 and reconstructed voxel size = 0.45 × 0.45 × 2, turbo spin-echo (TSE) factor = 43, sensitivity encoding (SENSE) factor = 2.5, and number of averages =1. The phase-encoding direction was the right-left direction, the half scan percentage of the k-space was 0.625, and the fat shift direction was towards the posterior. The overcontiguous slice thickness and relatively thick slice thickness were used to increase signal-to-noise ratio (SNR) in DIR images which have relatively low signal-to-noise ratio (SNR) because of the application of two consecutive inversion pulses. The scan time for the 3D DIR sequence was 6 min and 16 s.

In addition, isotropic sagittal structural 3D T1W images were acquired with a magnetization-prepared rapid acquisition of gradient echo (MPRAGE) sequence. The imaging parameters were as follows: TR/TE/TI =8.1/3.7/1013 ms, 8° flip angle, matrix =236 × 236, and voxel =1 × 1 × 1 mm³. To evaluate any brain abnormalities, T2-weighted images and fluid attenuated inversion recovery (FLAIR) images were also acquired.

Image processing and image analysis

Image processing was performed with Statistical Parametric Mapping-version 8 (SPM8) software (Wellcome Department of Imaging Neuroscience, University College, London, UK). DIR images and T1W images was segmented into gray matter, white matter, and others including CSF using the "New Segmentation" option in SPM8 software. Next, a study-specific T1W template was created from the segmented gray matter and white matter images using the "Diffeomorphic Anatomical Registration Through Exponentiated Lie Algebra (DARTEL)" algorithm (Ashburner 2007). This step resulted in six T1W templates and the deformation field maps for each T1 image. These processing steps were repeated for DIR images to create DIR templates and the deformation field maps for each subject. The next step was modulation to adjust for volume signal changes during normalization. Segmented DIR and T1W gray matter maps were warped to the study-specific 3D DIR template and T1W template, respectively, by multiplying the Jacobian determinants of the deformation fields that were obtained from the previously registered images using the "Normalize to MNI Space" option in SPM8 software. In the spatial smoothing step, we applied the Gaussian kernel of 8 × 8 × 8 mm full width at half-maximum (FWHM) for both the T1W tissue volume maps and DIR tissue volume maps.

Statistical analyses

The following voxel-based analyses were performed by using SPM8 software. First, to compare gray matter volumes among the CN, MCI, and AD groups, voxel-wise, one-way analysis of variance (ANOVA) tests with subject's age and gender as covariates were used for both DIR and T1WI methods, separately. Second, to directly compare gray matter volumes between DIR and T1W, voxel-wise paired t-test was used in each subject group. For both analyses, a significance level of $p = 0.01$ was applied with correction for multiple comparisons using the false discovery rate (FDR) method and clusters with at least 10 contiguous voxels for both gray matter volumes.

Furthermore, to conduct region-of-interest (ROI)-based comparisons of gray matter volume differences among the three groups for DIR and T1WI, ROI-based analysis was performed based on some predefined areas which are the well-known regions affected by AD pathology as well as regions showing significant differences in GMV among groups on the voxel-based analyses (Horinek et al. 2007; Sepulcre et al. 2013; Dai et al. 2009). Gray matter volumes were obtained from the right and left hippocampi and amygdalae, the posterior cingulate cortex, and the precuneus. These areas were automatically traced on the standard space using WFUPickAtlas software toolbox (http://fmri.wfubmc.edu/software/pickatlas), which generated atlas-based ROI regions. Analysis of covariance (ANCOVA) was used to test group differences in gray matter volumes with age and gender as covariates. Finally, the receiver operating characteristic (ROC) curve analysis was performed to demonstrate sensitivity and specificity of DIR and T1WI in the areas. MedCalc statistical software (http://www.medcalc.org/, Ostend, Belgium) was used to analyze the data. A significance level of $p = 0.05$ was applied for the ROI analysis.

Simulation study of T1W images

Because we used 4 mm slice thickness with using 2 mm overcontiguous slice thickness for DIR, we have a simulation study with using the T1W image to evaluate the observed effect of DIR due to contrast differences of DIR rather than not the different thick slice thickness. The T1W image was reconstructed with 2 mm and 4 mm slice thickness with keeping the same in-plane resolution to filter the T1W image to have the same slice thickness as the DIR image. Those filtered and interpolated T1W images were used the same processing pipeline as the original T1W image to evaluate the group differences of gray matter volumes among the three subject groups.

Results

Subject characteristics

The demographic data of the subjects are summarized in Table 1. Ages were not significantly different among the three groups ($p > 0.05$). Gender was not significantly different between the CN group and the other two groups ($p > 0.05$), but it was significantly different between the MCI and AD groups ($p < 0.05$). The Mini Mental State Examination (MMSE) scores were significantly different between the AD group and the other two groups ($p < 0.05$), but not between the MCI and CN groups ($p > 0.564$). Figure 1 shows the DIR (top row) images and T1W (bottom row) images created after DARTEL processing with segmented brain tissues.
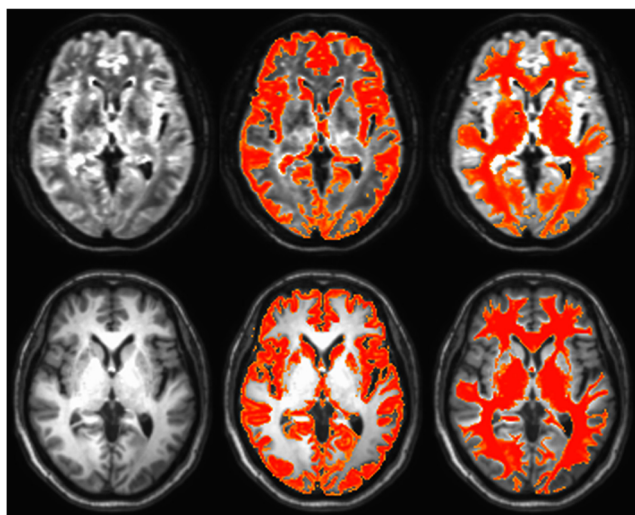

Fig. 1 Representative the three-dimensional double-inversion recovery (DIR) images (*top row*) and the three-dimensional T1-weighted images (*bottom row*) obtained from a subject and the corresponding segmentations of gray matter (*middle column*) and white matter (*rightmost column*)

GMV comparisons among the three groups for each imaging technique

Figure 2 shows the results of comparison of gray matter volumes between the CN and AD groups in the DIR images and T1W images of the brain. In the AD group compared with the CN group, the gray matter volume was decreased in both DIR and T1W images. However, the areas showing GMV loss were larger in DIR images compared to those in T1W images. Tables 2 and 3 present the locations showing significant differences in GMV on DIR and T1W images, respectively. The main areas showing GMV loss in the AD group compared with the CN group were as follows: the middle and inferior temporal gyrus, the right and left parahippocampal gyrus, the frontal gyrus, and the right and left precuneus.

Figure 3 shows the results of comparison of gray matter volumes between the MCI and AD groups in the DIR images and T1W images of the brain. In the AD group compared with the MCI group, the gray matter volume was decreased in both DIR and T1W images. However, the areas showing GMV loss were larger in DIR images compared to those in T1W images. Tables 2 and 3 present the locations showing significant differences in GMV on DIR and T1W images, respectively. The main areas showing GMV loss in the AD group compared with the MCI group were as follows: the left superior and middle temporal gyrus, and the right and left parahippocampal gyrus.

### GMV comparisons between the two imaging techniques for each subject group

Figure 4 shows the results of comparisons of gray matter volumes between DIR images and T1W images for each subject group. Blue color indicates greater GMV in DIR and red color indicates greater GMV in T1W. GMV in basal ganglia and neocortex was higher in T1W, but GMV in frontal and temporal areas was higher in DIR.

ROI-based analyses

Table 4 presents the mean and standard deviation (STD) of GMV at specific ROIs in the brain obtained from the T1W and DIR images in CN, MCI, and AD subjects. GMV was higher in DIR than in T1W in the CN and MCI groups. GMV was significantly different among the three groups for the hippocampi, amygdalae, and precuneus, except for the posterior cingulate cortex. GMV was significantly different between the two imaging techniques for the precuneus and both amygdalae, but not for both hippocampi and the posterior cingulate cortex.

The ROC curve analyses of GMV in the hippocampi (Fig. 5) and the amygdalae (Fig. 6) of the brain were

Fig. 2 Gray matter volume (GMV) loss in the patients with Alzheimer's disease (AD) compared with the cognitively normal (CN) elderly subjects on the three-dimensional double inversion recovery (DIR) and three-dimensional T1-weighted (T1W) images. *Red* color indicates decreased GMV in AD patients compared with CN subjects
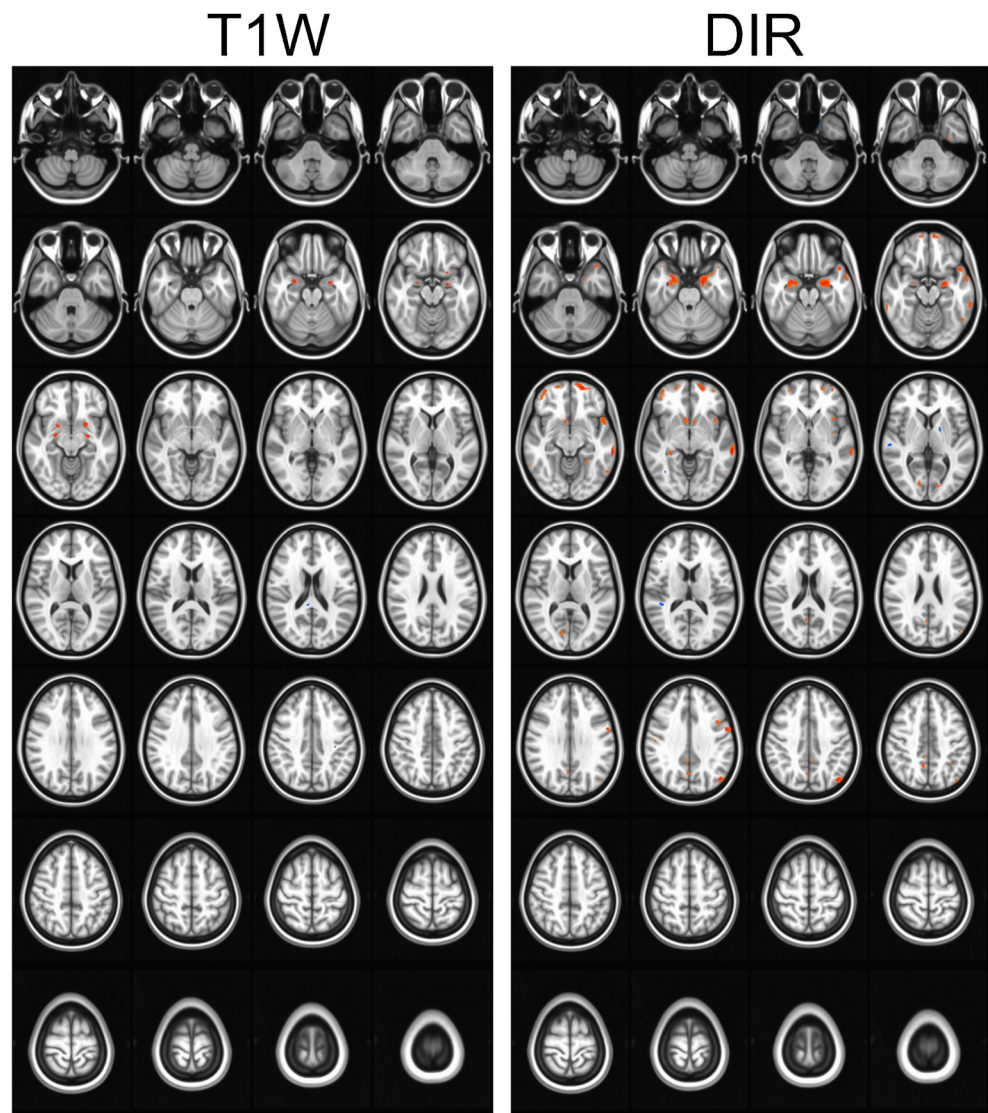
performed using T1W and DIR images in CN, MCI, and AD subjects. In the left hippocampi, the area under curve (AUC) values were higher in DIR than in T1W when we compared GMV values between the CN and AD groups ($p = 0.0152$). In the prescuneus, AUC values were also higher in DIR than in T1W when we compared GMV values between the MCI and AD groups ($p = 0.0339$). Amygdala had the highest AUC value for both DIR and T1W images. Those results are summarized in the supplemental table.

Simulation study of T1W images

The supplement figure shows the result of GMV differences among the three subject groups of T1W images with resampling 2 mm and 4 mm slice thicknesses. GMV in AD with 2 mm and 4 mm slice thickness was almost the same result as that with 1 mm slice thickness. In addition, when we increased the slice thickness of T1W image, we did not find additional

areas that showed significant GMV loss in AD. Furthermore, we did not find GMV loss in the frontal areas in the brain in AD compared with normal and MCI with 1 mm, 2 mm, and 4 mm slice thickness of T1W image. This simulation results indicated that the sequence itself was important to evaluate gray matter volume loss.

Discussion

With the rising prevalence of Alzheimer's disease, there is a pressing need for an imaging biomarker to evaluate the disease state and progression. Brain atrophy, assessed using volumetric MRI, is one of the imaging biomarkers in AD. It is therefore crucial to develop a sensitive technique to map brain tissue loss in order to understand AD. Since there is still no absolute cure for AD, detection of preclinical cases is important. Therefore, the purposes of this study were to

Table 2 Areas showing gray matter volume (GMV) loss in patients with Alzheimer's disease (AD) compared with cognitively normal (CN) elderly subjects and mild cognitive impairment (MCI) subjects in the three-dimensional double inversion recovery (DIR) images

Cluster size	Cluster location	BA	Talairach coordinates			z-score
AD < CN						
342	Lt Middle Temporal Gyrus	21	−60.23	−29.64	−6.76	5.29
228	Lt Middle Temporal Gyrus	39	−43.28	−72.78	29.98	4.87
464	Lt Superior Temporal Gyrus	38	−43.32	14.17	−13.13	4.65
	Lt Middle Temporal Gyrus	21	−52.6	3.04	−14.34	4.51
36	Rt Inferior Temporal Gyrus	20	57.38	−37.85	−13.65	4.31
33	Lt Inferior Temporal Gyrus	20	−54.71	−45.51	−8.17	4.19
69	Lt Fusiform Gyrus	37	−48.15	−54.07	−16.97	4.16
	Lt Inferior Temporal Gyrus	20	−52.86	−57.37	−11.96	4.13
11	Rt Inferior Temporal Gyrus	20	54.51	−49.54	−9.4	4.05
591	Lt Parahippocampal Gyrus	Amygdala	−20.2	−5.25	−17.28	5.26
417	Rt Parahippocampal Gyrus	Amygdala	25.16	−0.83	−16.1	4.86
67	Rt Parahippocampal Gyrus	27	26.76	−31.96	−5.5	4.45
	Rt Parahippocampal Gyrus	36	26.79	−38.13	−9.69	4.02
19	Lt Parahippocampal Gyrus	36	−25.06	−43.54	−10.18	3.96
76	Rt Lingual Gyrus	18	11.67	−75.11	3.66	4.16
32	Lt Lingual Gyrus	18	−15.13	−78.35	−0.7	4.09
	Lt Inferior Frontal Gyrus	47	−30.3	8.19	−19.78	4.04
408	Lt Superior Frontal Gyrus	11	−15.54	55.25	−1.56	5.16
163	Rt Inferior Frontal Gyrus		39.92	42.59	0.88	4.49
	Rt Middle Frontal Gyrus		35.31	51	1.6	4.35
147	Rt Medial Frontal Gyrus	10	17.74	54.82	1.66	4.25
	Rt Superior Frontal Gyrus	10	12.29	58.34	−5.3	4.18
52	Lt Middle Frontal Gyrus	10	−32.31	51.76	5.93	4.19
21	Rt Inferior Frontal Gyrus	47	40.03	18.74	−14.89	4.1
138	Lt Precentral Gyrus	6	−55.08	−4.36	32.66	4.66
35	Lt Precentral Gyrus	9	−40.26	5.72	34.77	4.44
10	Rt Postcentral Gyrus	2	46.67	−19.8	32.92	4.07
105	Rt Caudate, Head		6.51	10.07	−1.87	4.49
49	Lt Caudate, Head		−6.48	7.17	−0.56	4.04
39	Rt Posterior Cingulate	23	2.32	−57.47	15.99	4.46
164	Rt Precuneus	7	6.68	−54	38.01	4.42
	Rt Precuneus	31	1.21	−64.28	27.94	4.38
13	Lt Precuneus	31	−5.29	−48	34.77	3.92
70	Lt Claustrum		−36.11	12.65	2.16	4.18
22	Lt Claustrum		−34.34	−5.32	3.19	4.17
19	Lt Uncus	20	−28.36	−9.49	−31.33	4.12
15	Rt Cingulate Gyrus	31	3.95	−39.92	38.4	3.97
27	Rt Uvula		1.95	−61.59	−28.55	3.97
AD < MCI						
28	Lt Superior Temporal Gyrus	38	−48.78	6.6	−22.05	4.69
22	Lt Middle Temporal Gyrus	21	−60.22	−31.42	−7.83	4.5
13	Lt Superior Temporal Gyrus	38	−43.3	16.12	−13.85	4.46
17	Lt Fusiform Gyrus	37	−53.65	−48.11	−20.11	4.82
214	Lt Parahippocampal Gyrus	Amygdala	−23.03	−5.67	−12.87	5.63
247	Rt Parahippocampal Gyrus	Amygdala	23.27	−2.94	−13.63	5.4
	Rt Parahippocampal Gyrus	34	25.21	4.09	−18.33	4.42
27	Lt Precentral Gyrus	6	−55.08	−2.5	32.84	4.56

Table 2 (continued)

Cluster size	Cluster location	BA	Talairach coordinates			z-score
21	Rt Uncus	36	24.42	−2.23	−30.65	4.8
11	Lt Uncus	36	−25.56	−3.83	−31.65	4.54

AD Alzheimer's disease

CN cognitively normal elderly

BA Brodmann area

GM Gray matter

Z score Z-score in the local maxima

Lt. Left

Rt. Right

FDR False discovery rate

prospectively determine the sensitivity in the detection of brain tissue losses in AD patients compared with MCI or CN subjects using 3D DIR, and to compare the results with those obtained by tissue volume determinations using 3D T1WI at 3 T. The major findings of this study were; 1) DIR images were sensitive for identifying GMV loss in patients with AD compared with MCI and CN subjects, 2) areas showing GMV loss identified with DIR were similar to those identified with T1W, but they were extended to more brain areas, and 3) amygdala is the most important area to diagnose AD

and MCI. Therefore, the DIR sequence can be useful to characterize brain tissue alterations in patients with AD.

Whole brain analyses

DIR-based VBM was more sensitive for evaluating gray matter atrophy in AD than T1W-based VBM. Most of the atrophic regions identified with T1W-based VBM were also identified with DIR-based VBM. Furthermore, additional abnormalities were identified with DIR-based VBM. We applied the DIR

Table 3 Areas showing gray matter volume (GMV) loss in patients with Alzheimer's disease (AD) compared with cognitively normal (CN) elderly subjects and mild cognitive impairment (MCI) subjects in the three-dimensional T1-weighted (3D T1W) images

Cluster size	Cluster location	BA	Talairach coordinates			z-score
AD < CN						
107	Lt Parahippocampal Gyrus	Amygdala	−21.24	−8.83	−9.53	5.22
	Lt Parahippocampal Gyrus	Amygdala	−25.77	−3.53	−15.41	4.82
108	Rt Parahippocampal Gyrus	Amygdala	24.21	−2.86	−14.5	5.13
	Rt Lentiform Nucleus	Medial Globus Pallidus	19.46	−7.35	−6.9	5.11
30	Rt Lentiform Nucleus	Putamen	19.49	4.76	−5.75	4.85
96	Lt Lentiform Nucleus	Putamen	−20.27	7.01	−8.01	5.3
7	Lt Middle Temporal Gyrus	21	−62.09	−26.08	−4.65	4.64
AD < MCI						
105	Rt Lentiform Nucleus	Medial Globus Pallidus	19.49	−7.17	−8.68	5.67
87	Lt Parahippocampal Gyrus	Amygdala	−20.29	−6.88	−10.23	5.57
3	Rt Superior Temporal Gyrus	38	32.87	7.83	−37.67	4.64
2	Lt Middle Temporal Gyrus	21	−50.7	7.95	−16.55	4.62

AD Alzheimer's disease

CN Cognitively normal elderly

*BA* Brodmann area

GM Gray matter

Z score Z-score in the local maxima

Lt. Left

Rt. Right

FDR False discovery rate

Fig. 3 Gray matter volume (GMV) loss in the patients with Alzheimer's disease (AD) compared with the mild cognitive impairment (MCI) subjects on the three-dimensional double inversion recovery (DIR) and three-dimensional T1-weighted (T1W) images. *Red* color indicates decreased GMV in AD patients compared with MCI patients
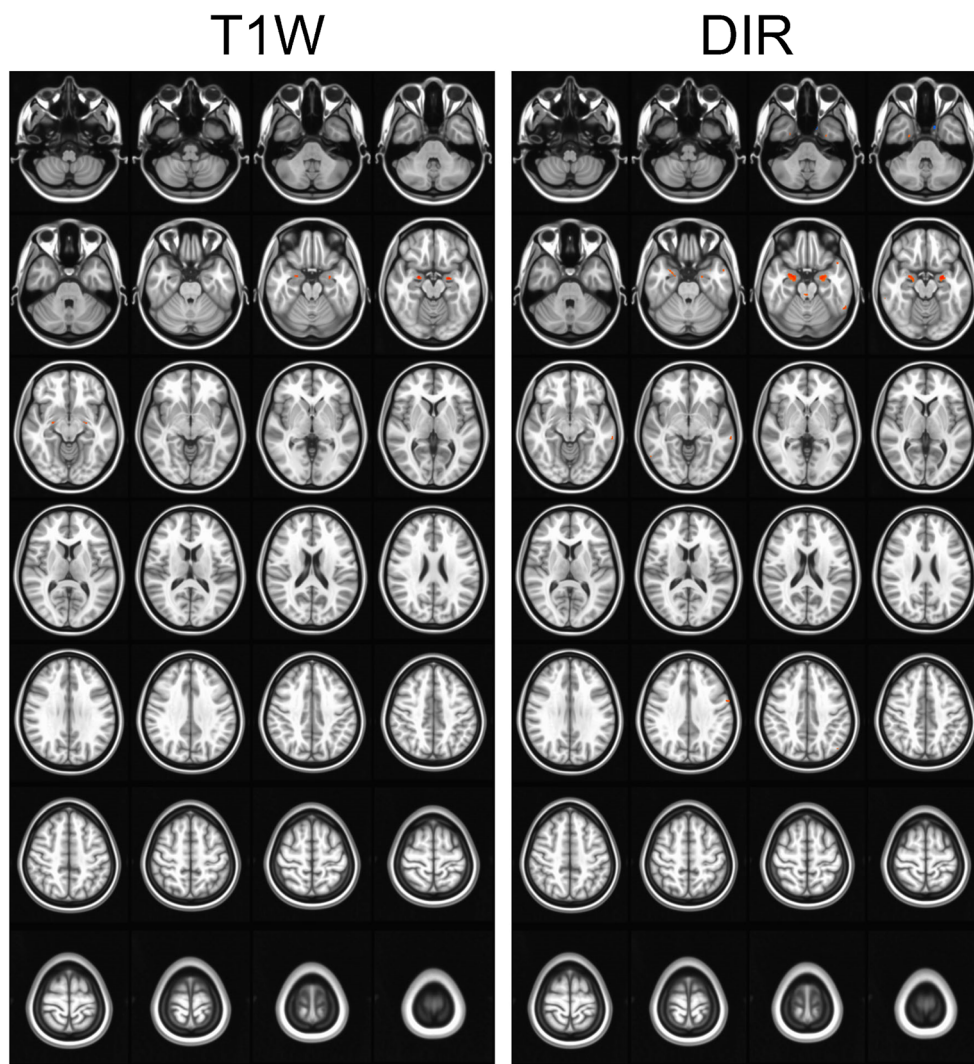
technique in patients with MCI and AD with a primary aim of assessing whether DIR could identify brain tissue alterations among groups. To the best of our knowledge, although previous studies focused on the diagnostic value of a DIR sequence concerning different applications in clinical neuroimaging (Pouwels et al. 2006; Turetschek et al. 1998; Morimoto et al. 2013b; Vural et al. 2013; Harris et al. 2013; Morimoto et al. 2013a; Li et al. 2011; Calabrese et al. 2007; Rugg-Gunn et al. 2006), this is the first application of DIR in patients with AD. The difference in T1 relaxation times among gray matter, white matter, and CSF allows suppression of one of these tissues in favor of selectively imaging the other tissue in the DIR method.

DIR at 3 T can detect brain tissue alterations especially in the temporal gyrus gray matter areas. The main atrophic areas were similar in both techniques, but these areas were extended to surrounding areas with DIR. Areas showing GMV loss on DIR images were much larger than those on T1W images, and the frontal areas of the brain were discriminated significantly with DIR, but not with T1W. Previous studies reported that

AD-associated brain atrophy usually begins in the temporal lobe, spreads to the posterior areas of the brain, and is finally apparent in the frontal areas in the late stage of AD (Baron et al. 2001; Bozzali et al. 2006). Therefore, frontal areas of the brain on DIR images may correctly reflect disease progression. This means that the sensitivity of DIR images in detecting GMV loss is higher than that of T1W images on comparison among the groups. Recently, T2-based VBM was introduced to evaluate regional atrophy in neurodegenerative disease (Diaz-de-Grenu et al. 2011). T2-based VBM technique was much more sensitive to atrophy detection than T1-based VBM. DIR is also one of the T2-weighted imaging techniques that selectively suppress two brain tissues, such as white matter and CSF. Therefore, DIR has the potential for early detection of whole brain atrophy in any neurodegenerative disease.

Most VBM studies have focused on abnormalities of gray matter distribution and have identified abnormalities of segmented gray matter in the brain. Accurate identification and classification of brain tissue and lesions are required to
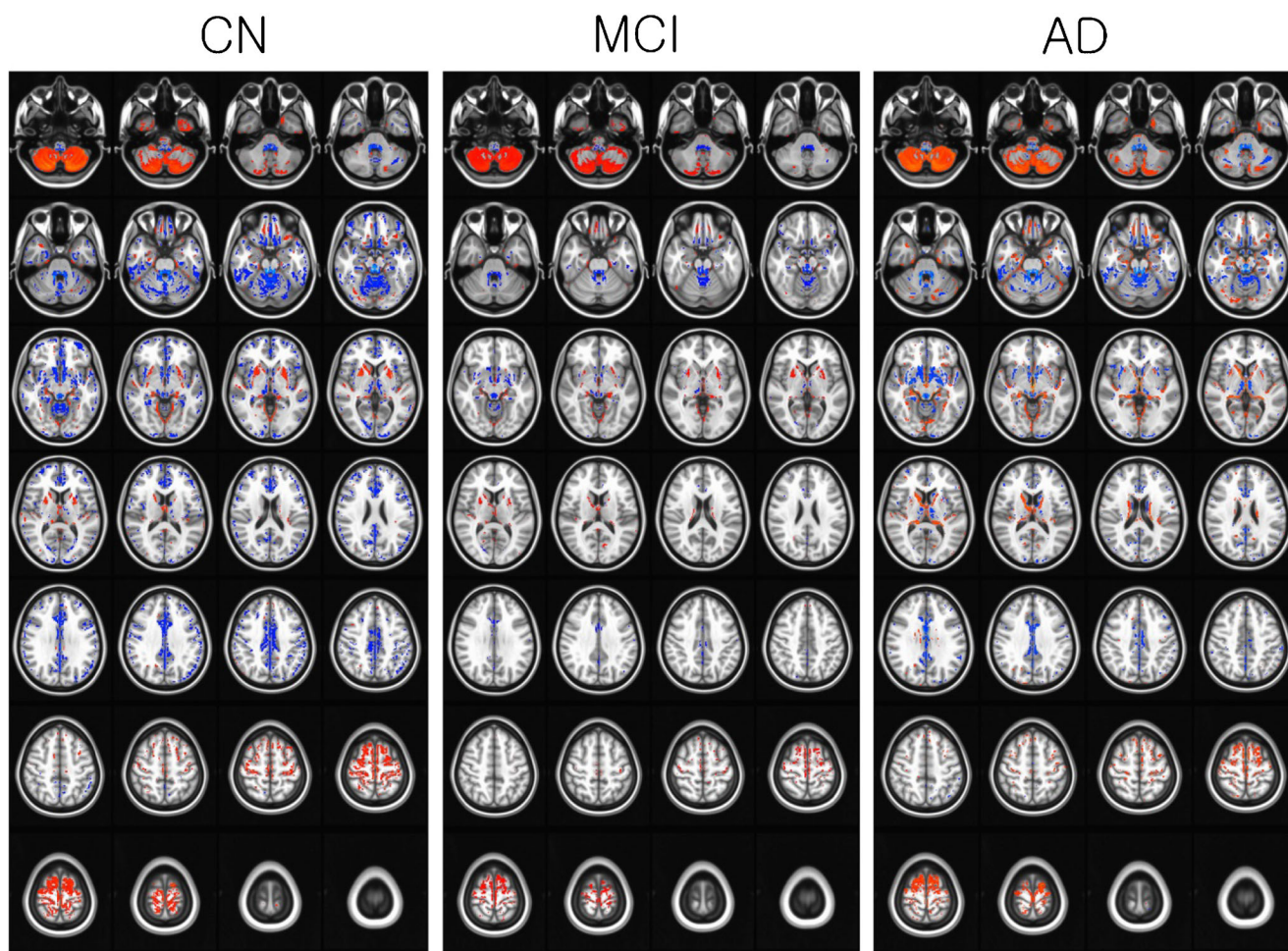
Fig. 4 Results of comparisons of gray matter volume (GMV) between three-dimensional double inversion recovery (DIR) and three-dimensional T1-weighted (T1W) images in cognitively normal (CN), mild cognitive impairment (MCI), and Alzheimer's disease (AD) subjects. *Blue* color indicates greater GMV in DIR and *red* color indicates greater GMV in T1W

understand the potential influence of the outcome. However, tissue segmentation is complicated in some cases. For example, the signal intensity of some white matter hyperintensities appears to be very close to that of normal gray matter in 3D T1W images, leading to misclassification of these white matter hyperintensities as gray matter with the use of some current MRI segmentation techniques. In addition, gray matter lesions are not detected routinely on conventional MR imaging. This is partly because of poor contrast between cortical lesions and the surrounding gray matter. This shortcoming limits the attempts to identify gray matter losses in some situations, and it can hinder understanding of the impact of cortical pathologic changes on clinical progression of the disease. This limitation may be minimized by using the 3D DIR images because neuronal loss will result in cortical atrophy and reduced gray matter signal intensity. Partial volume effects will play a role if the cortex is so thin that the contributing pixels only partly contain gray matter, causing lower signal intensity. For example, a voxel that contains 50 % gray matter, 25 % white matter, and 25 % CSF can be assumed to contain only gray matter

with DIR. The signal intensity in this voxel will be reduced to 50 % compared to that in a voxel that contains 100 % gray matter; however, the resulting image can be processed, assuming that only gray matter signal is present by removing the contaminated signal from the white matter and CSF. The advantage of the DIR technique can be applied to the white matter volume loss with suppression of both gray matter and CSF. However, DIR images may overestimate GMV loss because gray matter appears bright compared to suppressed CSF and white matter. Voxels containing small portion of gray matter may be regarded as voxels of gray matter and cause dilation of GMV. On visual assessment, GMV loss looks bigger in DIR images than in T1W images. This may additionally be related to use a relatively thick slice thickness in DIR compared to T1W. In addition, because spatial resolution of DIR in this study was lower than that in T1W, there may be more chances of partial volume artifacts in DIR compared to T1W. Therefore, further study should be performed to deal with overestimation of GMV in DIR by using a thin slice thickness and a high spatial resolution.

Table 4 Mean and standard deviation (STD) of gray matter volume (GMV) in the specific regions-of-interest (ROI) in the brain obtained from the three-dimensional T1-weighted (T1W) and double inversion recovery (DIR) images in cognitively normal (CN), mild cognitive impairment (MCI), and Alzheimer's disease (AD) subjects

ROI	Sequence (Seq)	Subject group (DDX) (mean ± STD)			Statistical result ANCOVA
		CN	MCI	AD	
Lt hippocampus	T1W	0.897 ± 0.030	0.900 ± 0.022	0.878 ± 0.032	DDX:F = 9.715, $p < 0.001$
	DIR	0.918 ± 0.032	0.916 ± 0.032	0.859 ± 0.055	Seq:F = 1.284, $p = 0.259$
Rt hippocampus	T1W	0.867 ± 0.054	0.871 ± 0.041	0.831 ± 0.046	DDX:F = 6.230, $p = 0.003$
	DIR	0.893 ± 0.081	0.905 ± 0.065	0.814 ± 0.090	Seq:F = 2.027, $p = 0.157$
Posterior cingulate	T1W	0.581 ± 0.030	0.595 ± 0.030	0.591 ± 0.025	DDX:F = 0.228, $p = 0.796$
	DIR	0.601 ± 0.025	0.591 ± 0.027	0.588 ± 0.027	Seq:F = 1.022, $p = 0.314$
Precuneus	T1W	0.518 ± 0.018	0.521 ± 0.016	0.517 ± 0.022	DDX:F = 7.391, $p = 0.001$
	DIR	0.564 ± 0.025	0.575 ± 0.027	0.546 ± 0.032	Seq:F = 122.134, $p < 0.001$
Lt amygdala	T1W	0.936 ± 0.015	0.938 ± 0.014	0.909 ± 0.020	DDX:F = 27.294, $p < 0.001$
	DIR	0.947 ± 0.019	0.956 ± 0.013	0.921 ± 0.024	Seq:F = 23.239, $p < 0.001$
Rt amygdala	T1W	0.932 ± 0.016	0.925 ± 0.016	0.891 ± 0.024	DDX:F = 32.368, $p < 0.001$
	DIR	0.955 ± 0.021	0.957 ± 0.019	0.924 ± 0.025	Seq:F = 81.410, $p < 0.001$

Mean represents average GMV over subject for each group

Analysis of covariance (ANCOVA) was used to test group differences in gray matter volumes with age and gender as covariates

To evaluate the accuracy of gray matter segmentations, Dice coefficient (Eggert et al. 2012) was calculated for both imaging techniques. Dice values were 0.793 ± 0.029 for CN, 0.803 ± 0.025 for MCI, and 0.794 ± 0.024 for AD groups. Furthermore, Jaccard similarity index was also calculated to measure similarity of gray matter volume between T1W and DIR. Jaccard index values were 0.658 ± 0.040 for CN, 0.671 ± 0.035 for MCI, and 0.660 ± 0.033 for AD groups. The accuracy of gray matter segmentation was about 80 %, but similarity of segmentation was about 66 %. The problem in the calculation of Dice coefficient in this study was that there was no standard gray matter segmentation reference. Therefore, the DC value was the relative value between the two imaging techniques.

Amygdala is the most sensitive area to differentiate among subject groups

Both DIR and T1W images showed gray matter volume loss in the amygdala in AD patients compared with MCI and CN subjects. This result was consistent with previous reports (Baron et al. 2001; Guo et al. 2010; Horinek et al. 2007). GMV in both amygdalae was significantly lower in AD patients compared with MCI and CN subjects and it was significantly higher with DIR than with T1W (Table 4). Amygdala had the highest AUC value for both DIR and T1W images. Therefore, amygdala GMV was the most sensitive imaging biomarker to differentiate AD and MCI patients from CN subjects. Hippocampal GMV was the second most sensitive imaging biomarker. Hippocampal GMV showed significant differences among subject groups, but not between the two

imaging techniques. In addition, DIR images revealed decreased GMV of the right precuneus in AD patients compared with MCI patients, but T1W images did not show this finding. Precuneal GMV was also significantly different between the two imaging techniques. Overall, the DIR technique can be used to obtain GMV as an imaging biomarker to differentiate AD patients from CN and MCI subjects.

Regional difference of gray matter volume between DIR and T1W images

In this study, we found that GMV in the basal ganglia and neocortex was higher in T1W, but that in the frontal and temporal areas was higher in DIR. The neocortex area has high curvature and complicated gyri and sulci with the deep infolding of the cerebral sulci. Therefore, the thin slice in T1W without blurring imaging quality may be better in quantification of gray matter volume in the neocortex area than DIR which is somewhat blurred in general compared to T1W. The thick slice thickness in DIR can also cause partial volume effect in the cortex area. In addition, the gyri and sulci with the thin and deep folded cortex areas may have regional variations in cortical T1 relaxation time, causing imperfect suppression of white matter and/or partially suppressed gray matter.

In the temporal areas, higher GMV of DIR than T1W may be related to reduce signal contributions from white matter in DIR. Signal intensity in the voxel which has mixed both gray matter and white matter come from gray matter only in DIR (assuming a perfect suppression both CSF and white matter), but do from both gray matter and white matter in T1W
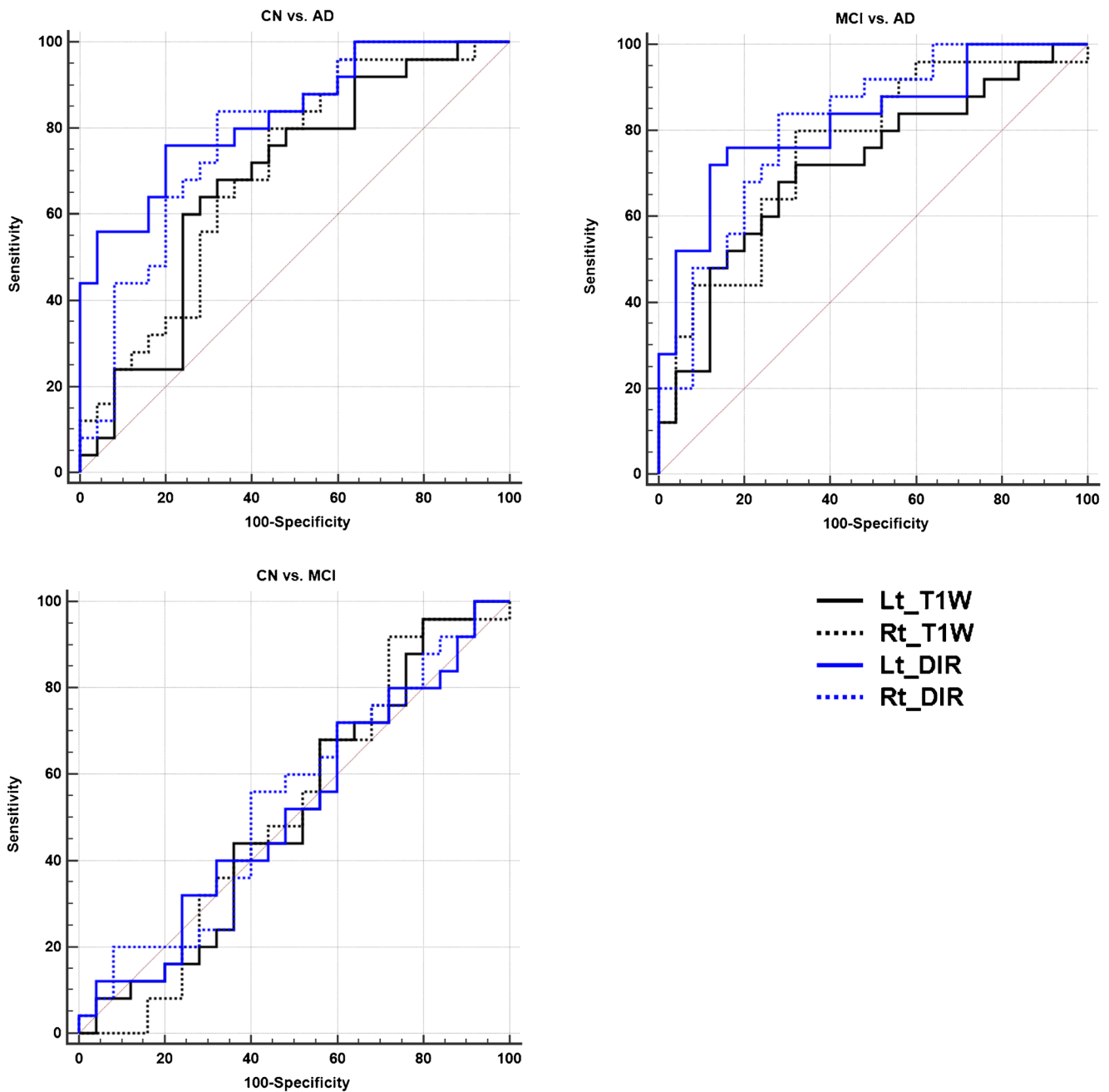
Fig. 5 Graphs of the receiver operating characteristic (ROC) curve analysis of gray matter volume (GMV) in the left and right hippocampi in the brain obtained from three-dimensional (3D) T1-weighted (T1W) and double inversion recovery (DIR) images in cognitively normal (CN), mild cognitive impairment (MCI), and Alzheimer's disease (AD) subjects. Area under the curve (AUC) values were higher in DIR than in T1W when we compared GMV values between CN and AD subjects in the left hippocampi ($p = 0.0152$)

(assuming a perfect suppression of CSF). GVM in T1W, therefore, depends on the result of white matter segmentation. Furthermore, B0 field inhomogeneity in the temporal area is greater in T1W acquired with a gradient-echo sequence than in DIR based on a spin-echo sequence. Field inhomogeneity in the frontal area is also greater in T1W than in DIR. This may be also affected in gray matter segmentation in T1W images and therefore can affect the quantification of gray matter volume.

Study limitations

There were several limitations to this study. First, we did not verify which results with DIR or T1W are more close to real tissue alterations. To verify this issue, we should perform a cadaver study in the brain removed during autopsy. Second, a DIR sequence should be developed to improve temporal and spatial resolution with minimization of flow-related artifact. In this study, we did not consider these points. The slice thickness
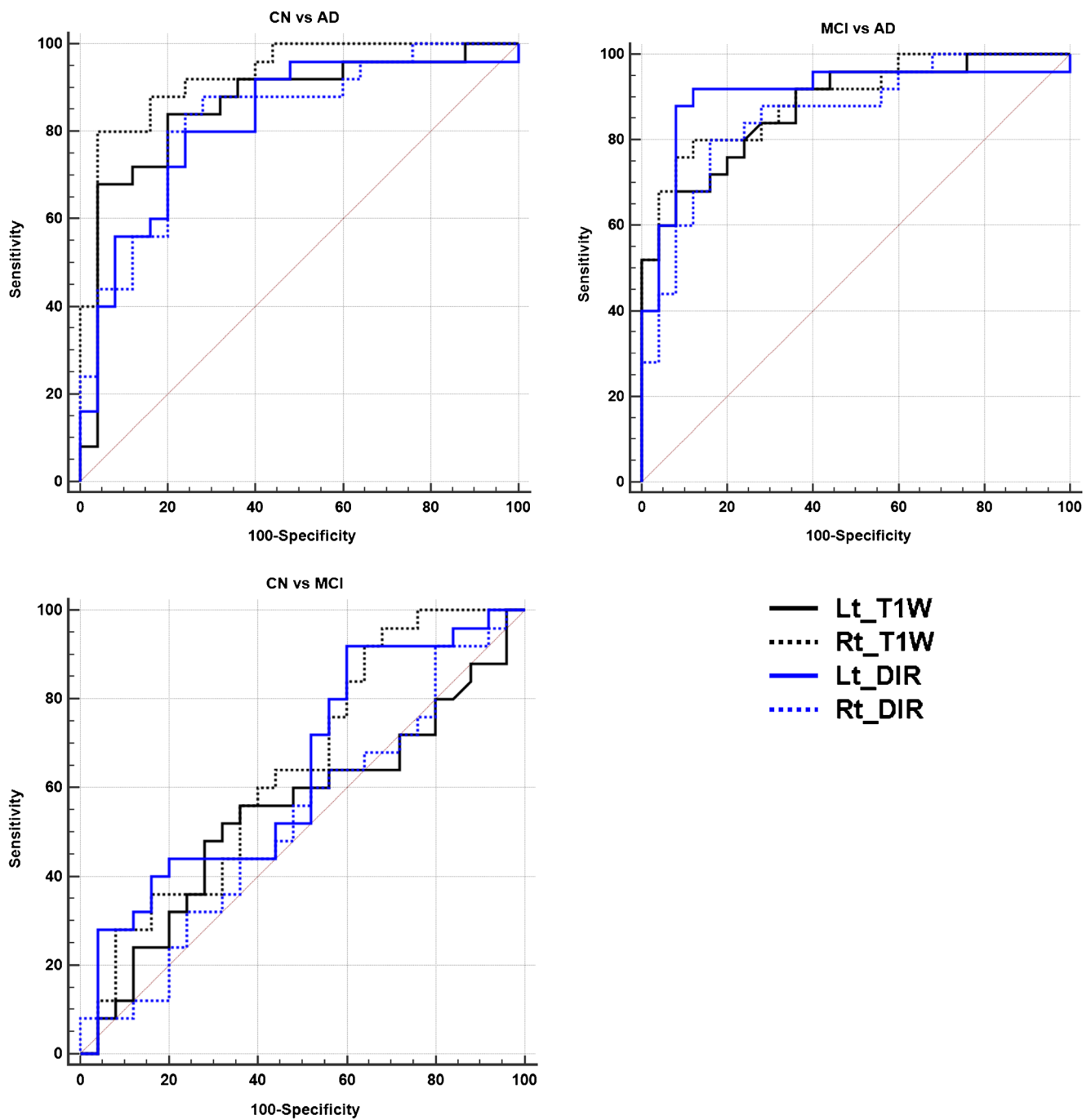
Fig. 6 Graphs of the receiver operating characteristic (ROC) curve analysis of gray matter volume (GMV) in the left and right amygdalae in the brain obtained from three-dimensional (3D) T1-weighted (T1W) and double inversion recovery (DIR) images in cognitively normal (CN), mild cognitive impairment (MCI), and Alzheimer's disease (AD) subjects

was 4 mm with using overcontiguous 2 mm slice thickness which might be too thick to estimate gray matter volume in the brain cortex. In the next study, we recommend to have a verification study with using a thin slice thickness. Increasing voxel resolution can be increased scan duration which causes to produce motion related-artifact in AD patients. Finally, in order to verify the results of this work, additional studies including more number of subjects should be performed.

Conclusions

DIR images were sensitive for identifying GMV loss in patients with AD compared with MCI and CN subjects and areas showing GMV loss identified with DIR were similar to those identified with T1W, but they were extended to more brain areas. With DIR, amygdala GMV is the most sensitive in differentiating between subject groups and it can be used as

a new imaging biomarker. DIR imaging can be useful for the evaluation of brain tissue volume in patients with neurodegenerative diseases.

References

Ahn, H. J., Chin, J., Park, A., Lee, B. H., Suh, M. K., Seo, S. W., et al. (2010). Seoul neuropsychological screening battery-dementia version (SNSB-D): a useful tool for assessing and monitoring cognitive impairments in dementia patients. *Journal of Korean Medical Science*, 25(7), 1071–1076. doi:10.3346/jkms.2010.25.7.1071.

Ashburner, J. (2007). A fast diffeomorphic image registration algorithm. *NeuroImage*, 38(1), 95–113. doi:10.1016/j.neuroimage.2007.07.007.

Ashburner, J., & Friston, K. J. (2000). Voxel-based morphometry–the methods. *NeuroImage*, 11(6 Pt 1), 805–821. doi:10.1006/nimg.2000.0582.

Baron, J. C., Chetelat, G., Desgranges, B., Perchey, G., Landeau, B., de la Sayette, V., et al. (2001). In vivo mapping of gray matter loss with voxel-based morphometry in mild Alzheimer's disease. *NeuroImage*, 14(2), 298–309. doi:10.1006/nimg.2001.0848.

Boulby, P. A., Symms, M. R., & Barker, G. J. (2004). Optimized interleaved whole-brain 3D double inversion recovery (DIR) sequence for imaging the neocortex. *Magnetic Resonance in Medicine*, 51(6), 1181–1186. doi:10.1002/mrm.20088.

Bozzali, M., Filippi, M., Magnani, G., Cercignani, M., Franceschi, M., Schiatti, E., et al. (2006). The contribution of voxel-based morphometry in staging patients with mild cognitive impairment. *Neurology*, 67(3), 453–460. doi:10.1212/01.wnl.0000228243.56665.c2.

Calabrese, M., De Stefano, N., Atzori, M., Bernardi, V., Mattisi, I., Barachino, L., et al. (2007). Detection of cortical inflammatory lesions by double inversion recovery magnetic resonance imaging in patients with multiple sclerosis. *Archives of Neurology*, 64(10), 1416–1422. doi:10.1001/archneur.64.10.1416.

Dai, W., Lopez, O. L., Carmichael, O. T., Becker, J. T., Kuller, L. H., & Gach, H. M. (2009). Mild cognitive impairment and Alzheimer disease: patterns of altered cerebral blood flow at MR imaging. *Radiology*, 250(3), 856–866. doi:10.1148/radiol.2503080751.

Diaz-de-Grenu, L. Z., Acosta-Cabronero, J., Pereira, J. M., Pengas, G., Williams, G. B., & Nestor, P. J. (2011). MRI detection of tissue pathology beyond atrophy in Alzheimer's disease: introducing T2-VBM. *NeuroImage*, 56(4), 1946–1953. doi:10.1016/j.neuroimage.2011.03.082.

Eggert, L. D., Sommer, J., Jansen, A., Kircher, T., & Konrad, C. (2012). Accuracy and reliability of automated gray matter segmentation pathways on real and simulated structural magnetic resonance images of the human brain. *PloS One*, 7(9), e45081. doi:10.1371/journal.pone.0045081.

Good, C. D., Scahill, R. I., Fox, N. C., Ashburner, J., Friston, K. J., Chan, D., et al. (2002). Automatic differentiation of anatomical patterns in the human brain: validation with studies of degenerative dementias. *NeuroImage*, 17(1), 29–46. doi:10.1006/nimg.2002.1202.

Guo, X., Wang, Z., Li, K., Li, Z., Qi, Z., Jin, Z., et al. (2010). Voxel-based assessment of gray and white matter volumes in Alzheimer's disease. *Neuroscience Letters*, 468(2), 146–150. doi:10.1016/j.neulet.2009.10.086.

Harris, R. J., Cloughesy, T. F., Pope, W. B., Godinez, S., Natsuaki, Y., Nghiemphu, P. L., et al. (2013). Pre- and post-contrast three-dimensional double inversion-recovery MRI in human glioblastoma. *Journal of Neuro-Oncology*, 112(2), 257–266. doi:10.1007/s11060-013-1057-y.

Horinek, D., Varjassyova, A., & Hort, J. (2007). Magnetic resonance analysis of amygdalar volume in Alzheimer's disease. *Current Opinion in Psychiatry*, 20(3), 273–277. doi:10.1097/YCO.0b013e3280ebb613.

Li, Q., Zhang, Q., Sun, H., Zhang, Y., & Bai, R. (2011). Double inversion recovery magnetic resonance imaging at 3 T: diagnostic value in hippocampal sclerosis. *Journal of Computer Assisted Tomography*, 35(2), 290–293. doi:10.1097/RCT.0b013e3182073c56.

McKhann, G., Drachman, D., Folstein, M., Katzman, R., Price, D., & Stadlan, E. M. (1984). Clinical diagnosis of Alzheimer's disease: report of the NINCDS-ADRDA work group under the auspices of department of health and human services task force on Alzheimer's disease. *Neurology*, 34(7), 939–944.

Meara, S. J., & Barker, G. J. (2005). Evolution of the longitudinal magnetization for pulse sequences using a fast spin-echo readout: application to fluid-attenuated inversion-recovery and double inversion-recovery sequences. *Magnetic Resonance in Medicine*, 54(1), 241–245. doi:10.1002/mrm.20541.

Morimoto, E., Kanagaki, M., Okada, T., Yamamoto, A., Mori, N., Matsumoto, R., et al. (2013a). Anterior temporal lobe white matter abnormal signal (ATLAS) as an indicator of seizure focus laterality in temporal lobe epilepsy: comparison of double inversion recovery, FLAIR and T2W MR imaging. *European Radiology*, 23(1), 3–11. doi:10.1007/s00330-012-2565-4.

Morimoto, E., Okada, T., Kanagaki, M., Yamamoto, A., Fushimi, Y., Matsumoto, R., et al. (2013b). Evaluation of focus laterality in temporal lobe epilepsy: a quantitative study comparing double inversion-recovery MR imaging at 3 T with FDG-PET. *Epilepsia*. doi:10.1111/epi.12396.

Petersen, R. C., Smith, G. E., Waring, S. C., Ivnik, R. J., Tangalos, E. G., & Kokmen, E. (1999). Mild cognitive impairment: clinical characterization and outcome. *Archives of Neurology*, 56(3), 303–308.

Petersen, R. C., Doody, R., Kurz, A., Mohs, R. C., Morris, J. C., Rabins, P. V., et al. (2001). Current concepts in mild cognitive impairment. *Archives of Neurology*, 58(12), 1985–1992. doi:10.1001/archneur.58.12.1985.

Pouwels, P. J., Kuijer, J. P., Mugler 3rd, J. P., Guttmann, C. R., & Barkhof, F. (2006). Human gray matter: feasibility of single-slab 3D double inversion-recovery high-spatial-resolution MR imaging. *Radiology*, 241(3), 873–879. doi:10.1148/radiol.2413051182.

Redpath, T. W., & Smith, F. W. (1994). Technical note: use of a double inversion recovery pulse sequence to image selectively grey or white brain matter. *The British Journal of Radiology*, 67(804), 1258–1263.

Rugg-Gunn, F. J., Boulby, P. A., Symms, M. R., Barker, G. J., & Duncan, J. S. (2006). Imaging the neocortex in epilepsy with double inversion recovery imaging. *NeuroImage*, 31(1), 39–50. doi:10.1016/j.neuroimage.2005.11.034.

Sepulcre, J., Sabuncu, M. R., Becker, A., Sperling, R., & Johnson, K. A. (2013). In vivo characterization of the early states of the amyloid-beta network. *Brain*, *136*(Pt 7), 2239–2252. doi:10.1093/brain/awt146.

Small, G. W., Bookheimer, S. Y., Thompson, P. M., Cole, G. M., Huang, S. C., Kepe, V., et al. (2008). Current and future uses of neuroimaging for cognitively impaired patients. *Lancet Neurology*, *7*(2), 161–172. doi:10.1016/S1474-4422(08)70019-X.

Turetschek, K., Wunderbaldinger, P., Bankier, A. A., Zontsich, T., Graf, O., Mallek, R., et al. (1998). Double inversion recovery imaging of the brain: initial experience and comparison with fluid attenuated inversion recovery imaging. *Magnetic Resonance Imaging*, *16*(2), 127–135. doi:10.1016/S0730-725X(97)00254-3.

Vural, G., Keklikoglu, H. D., Temel, S., Deniz, O., & Ercan, K. (2013). Comparison of double inversion recovery and conventional magnetic resonance brain imaging in patients with multiple sclerosis and relations with disease disability. *The Neuroradiology Journal*, *26*(2), 133–142. doi:10.1177/197140091302600201.